Hindawi Publishing Corporation
Journal of Chemistry
Volume 2015, Article ID 635281, 7 pages
http://dx.doi.org/10.1155/2015/635281

Research Article

Three-Dimensional Modeling of Hydrodynamics and Biokinetics in EGSB Reactor

Jixiang Yang,[1] Yanqing Yang,[1,2] Xin Ji,[1,2] Youpeng Chen,[1] Jinsong Guo,[1] and Fang Fang[2]

[1]*Key Laboratory of Reservoir Aquatic Environment, Chongqing Institute of Green and Intelligent Technology, Chinese Academy of Sciences, Chongqing 400714, China*
[2]*School of Urban Construction and Environmental Engineering, Chongqing University, Chongqing 400030, China*

Correspondence should be addressed to Fang Fang; fangfangcq@cqu.edu.cn

Received 9 April 2015; Accepted 15 June 2015

Academic Editor: Ghadir A. El-Chaghaby

A three-dimensional model integrating computational fluid dynamics (CFD) and biokinetics was established to model an expanded granular sludge bed (EGSB) reactor in this study. The EGSB reactor treating synthesized municipal wastewater was operated at ambient temperature. The model provided satisfactory modeling results regarding hydrodynamics and biokinetics. The model shows that influent distribution was evenly distributed. In addition, butyrate and propionate degradation rates linearly decreased along the flow direction in the reactor. However, acetate degradation rate increased first and decreased later. VFA degradation rate distributions were different at each reactor cross section. VFA degradation rates near reactor wall were lower than VFA degradation rates at reactor axis. Moreover, a pulse high influent COD concentration had a tiny impact on effluent quality, which indicates that the reactor was stable while treating synthesized wastewater at adopted conditions.

1. Introduction

Expanded granular sludge bed (EGSB) is a granular sludge-based wastewater treatment technology and has been widely applied in high strength wastewater treatment. In addition, many researches regarding low strength wastewater treatment, that is, municipal wastewater treatment, have been reported [1–3].

Vertical slim columns are applied as structures of EGSB reactors. However, a staged reactor structure resulted in a more efficient reactor [4], which indicates that there is a need for the optimization of EGSB reactor structure. The optimization requires insight of hydrodynamics as well as biokinetics in EGSB reactors. The hydrodynamics and biokinetics in upflow anaerobic sludge blanket (UASB) were analyzed, which resulted in a model integrating hydrodynamics and biokinetics [5]. However, the integrated model was too complex and parameterized.

Alternatively, by the application of computational fluid dynamics (CFD), the hydrodynamics as well as mass transfer in EGSB reactors could be well obtained. Up to now, a few works applying two-dimensional (2D) CFD models have been reported [6–9]. However, if a flow field is too complex to be simplified as a 2D model, a three-dimensional (3D) CFD model is required. Considering the complexity of flow near the inlet of an EGSB reactor, it could be better to apply a 3D CFD model. Regarding 3D CFD models, a few reports about continual stirred flow reactors and aerobic bioreactors as well as anaerobic digesters were reported [10–13]. Nevertheless, reports regarding 3D CFD models about EGSB reactors are still not available.

Moreover, while hydrodynamics and biokinetic are needed to be integrated, it is considered that a 3D hydrodynamic model is better to be applied than applying a 2D CFD model. That is because real mass transfer conditions can be better modelled. After extensive 3D CFD modelling work regarding anaerobic digesters having been done, flow and biokinetics in anaerobic digesters are well known [7, 14–16]. Nevertheless, these researches were not related to EGSB reactors.

Influent distribution is considered playing an important role in reactor operations and especially essential at large scales. If influent distribution is required to be included in a CFD model, a 3D rather than a 2D CFD model is required.

Table 1: Biokinetic applied in the integrated model [26].

	S_{bu}	S_{pro}	S_{ac}	Reaction rate
Butyrate degradation	−1		$0.8(1 - Y_{bu})$	$k_{m\_bu} \cdot S_{bu} \cdot X/(K_{s\_bu} + S_{bu})$
Propionate degradation		−1	$0.57(1 - Y_{pro})$	$k_{m\_pro} \cdot S_{pro} \cdot X/(K_{s\_pro} + S_{pro})$
Acetate degradation			−1	$k_{m\_ac} \cdot S_{ac} \cdot X/(K_{s\_ac} + S_{ac})$

Table 2: The parameters applied in the biokinetic models (26°C).

K_{s_bu}	Half-saturation constant for butyrate	15	g COD/m^3
K_{s_pro}	Half-saturation constant for propionate	10	g COD/m^3
K_{s_ac}	Half-saturation constant for acetate	60	g COD/m^3
Y_{bu}	Yield for butyrate utilization	0.066	COD/COD
Y_{pro}	Yield for propionate utilization	0.050	COD/COD
Y_{ac}	Yield for acetate utilization	0.032	COD/COD
k_{m_bu}	Maximum butyrate utilization rate	0.76	g COD/g VSS·d
k_{m_pro}	Maximum propionate utilization rate	0.53	g COD/g VSS·d
k_{m_ac}	Maximum acetate utilization rate	1.75	g COD/g VSS·d
S_{bu}	Concentration of butyrate		mg/L
S_{pro}	Concentration of propionate		mg/L
S_{ac}	Concentration of acetate		mg/L

A 2D model can only be applied to model a reactor that is built in an axisymmetric structure. However, the distribution plate located at the bottom of the EGSB reactor made the reactor not axisymmetric. This study aimed at establishing a 3D CFD model regarding a EGSB reactor. In the model, water distribution was not assumed to be uniform and was included in the model. In addition, the model integrated anaerobic biokinetics, which was beneficial to obtain details regarding reactor operation such as influent distribution and reaction rates distribution.

2. Methods and Materials

2.1. EGSB Operation. Peristalsis pumps (Jihpump BT-100EA, China) were applied for providing influent and backflow to a lab scale EGSB reactor. Hydraulic retention time was 2.5 hours and upflow velocity was maintained at 5 m/h. Inoculum sludge was taken from an internal circulation reactor treating pulping wastewater (Chongqing, China). The EGSB reactor was fed with synthetic wastewater prepared by volatile fatty acids (VFA). The chemical oxygen demand (COD) ratio of acetate : propionate : butyrate was 2 : 1 : 1 while total COD concentration of the influent was between 350 and 430 mg/L. Ammonium concentration and phosphate concentration were 30 mg/L and 4 mg/L, respectively. $NaHCO_3$ was applied to maintain pH between 6.8 and 7.5. During the operation of the reactor, volatile suspended solid (VSS) was measured by standard method [17]. VFA were measured by high pressured liquid chromatography (DIONEX Ultimate 3000 HPLC, USA). The reactor was operated at 26°C.

2.2. EGSB Modelling

2.2.1. Included Biokinetics. After operating the reactor for 75 days, effluent COD and the height of sludge bed were stable. VSS concentration decreased along the flow direction in the reactor and is given by

$$X = (88.32 - 1.92 * h) \times 1000, \quad (1)$$

where X is concentration of VSS, mg/L; h is reactor height, 0~46 cm.

VFA were degraded in the sludge bed. Therefore, three bioprocesses shown in Tables 1 and 2 were included in the integrated model. VSS concentrations shown in (1) were included and were constant in the integrated model. Therefore, biomass decay and growth were not necessary to be included in the applied biokinetics.

2.2.2. Model Geometry. In the EGSB reactor, a sedimentation zone (free flow zone) and a sludge bed right under the sedimentation zone were observed. COD was degraded in the sludge bed and almost no COD degradation took place in the sedimentation zone. In this model, the sludge bed was treated as a porous bed and no reaction occurred in the sedimentation zone. Two different modeling domains, that required different model strategies, are shown in Figure 1.

2.2.3. Meshing. The modelling domains were meshed in COMSOL Multiphysics (version 4.3 a) that was the model platform of this study. Average element quality was 0.52 cm while the minimum element quality was 0.0058 cm. The meshing was sufficiently fine and did not have an impact on modelling results.

2.2.4. Hydrodynamics and Mass Transport Modeling. As shown in (1), sludge concentrations at different locations in the EGSB reactor were different, which is different from well mixed anaerobic digesters and aerobic bioreactors [10–13]. Sludge concentration has a big impact on sludge viscosity,

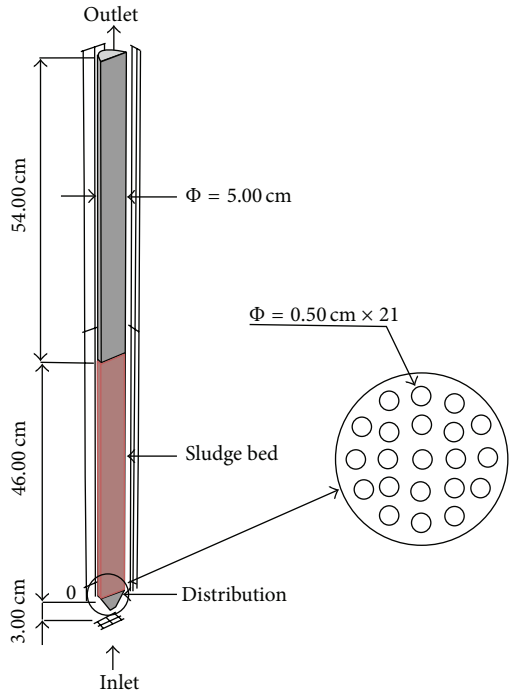

Figure 1: Schematic view of the modelling domains.

which made sludge a non-Newtonian liquid [18]. However, water in the free flow zone was a Newtonian liquid. Therefore, influent flowed into a non-Newtonian phase and a Newtonian liquid consequently, which resulted in a modeling difficulty. Nevertheless, sludge bed can be treated as a porous bed while influent flowed in space between sludge particles. By this kind of treatment, it was not the sludge viscosity but sludge bed porosity and permeability had impacts on flow in the sludge bed because water and sludge particles were separated rather than treated as a single phase. By this kind of simplification, influent could continuously flow into and out of the sludge bed and then into the free flow zone.

The porosity and permeability of sludge bed were calculated by (2) and (3), respectively;

$$\varepsilon_p = \frac{\rho_g - \rho_t}{\rho_g - \rho_w}, \tag{2}$$

$$\kappa = \nu \frac{\mu \Delta x}{\Delta p}, \tag{3}$$

where ε_p is porosity; ρ_g is wet granular density, kg/m^3; ρ_t is sludge bed density, kg/m^3; ρ_w is water density, kg/m^3; κ is permeability, m^2; ν is wastewater superficial velocity, m/s; Δx is sludge bed height, m; Δp is pressure different across sludge bed height, Pa; μ is water viscosity, Pa/s.

In the sedimentation zone, limited sludge existed and the zone was a free flow zone. Navier-Stokes equations ((4)-(5)) were applied to model the flow in the free flow zone. As for the mass convection and diffusion, (6) was applied in the free flow zone and sludge bed. Sludge bed was treated as a porous bed in the model. Brinkman equations ((7)-(8)) were applied to model hydraulic dynamics in the sludge bed.

Continuity in the free flow zone is as follows:

$$\frac{\delta \rho}{\delta t} + \nabla (\rho u) = 0. \tag{4}$$

Momentum in the free flow zone is as follows:

$$\rho \frac{\delta \mathbf{u}}{\delta t} + \rho \mathbf{u} \nabla \mathbf{u} = -\nabla p + \nabla \left[\mu \left(\mathbf{u} + (\nabla \mathbf{u})^T \right) - \frac{2}{3} \mu (\nabla \mathbf{u}) \mathbf{I} \right] + \mathbf{F}. \tag{5}$$

Mass convection and diffusion are as follows:

$$\frac{\delta c}{\delta t} + u \nabla c = \nabla (D \nabla c) + R. \tag{6}$$

Continuity in the sludge bed is as follows:

$$\frac{\delta \left(\varepsilon_p \rho \right)}{\delta t} + \nabla (\rho \mathbf{u}) = Q_{br}. \tag{7}$$

Momentum in the sludge bed is as follows:

$$\frac{\rho}{\varepsilon_p} \left(\frac{\delta \mathbf{u}}{\delta t} + (\mathbf{u} \nabla) \frac{\mathbf{u}}{\varepsilon_p} \right) = -\nabla p + \nabla \left\{ \frac{1}{\varepsilon_p} \left[\mu \left(\mathbf{u} + (\nabla \mathbf{u})^T \right) - \frac{2}{3} \mu (\nabla \mathbf{u}) \mathbf{I} \right] \right\} - \left(\frac{\mu}{\kappa} + \frac{Q_{br}}{{\varepsilon_p}^2} \right) \mathbf{u} + \mathbf{F}, \tag{8}$$

where c is concentration of species, mol/m^3; D is diffusion coefficient, m^2/s; R is reaction rate expression for the species, mol/(m^3·s); $\mathbf{u}$ is the velocity vector, m/s; ρ is density of the fluid, kg/m^3; p is pressure, Pa; Q_{br} is a mass source or mass sink, kg/(m^3·s); $\mathbf{F}$ is volume force, N/m^3; $\mathbf{I}$ is unit matrix.

2.2.5. Boundary Conditions. Inlet boundary condition was velocity inlet, while pressure and no viscous stress boundary condition was applied to the outlet. The latter boundary condition corresponds to (9). At the outlet, convection and migration were the governing mass transport mechanisms and diffusion transport was ignored:

$$\left[\mu \left(\nabla \mathbf{u} + (\nabla \mathbf{u})^T \right) \right] \cdot \mathbf{n} = 0, \tag{9}$$

where $\mathbf{n}$ is a unit vector.

2.2.6. Solver and Converge Conditions. Stationary solver was applied to solve the integrated model. The solution converged while residual errors for pressure, momentum, and species concentrations were below 0.001.

2.2.7. Tracer Experiments. The hydrodynamics and convection-diffusion of mass in the model were verified by applying $CaCl_2$ as a tracer. $CaCl_2$ was injected into the reactor

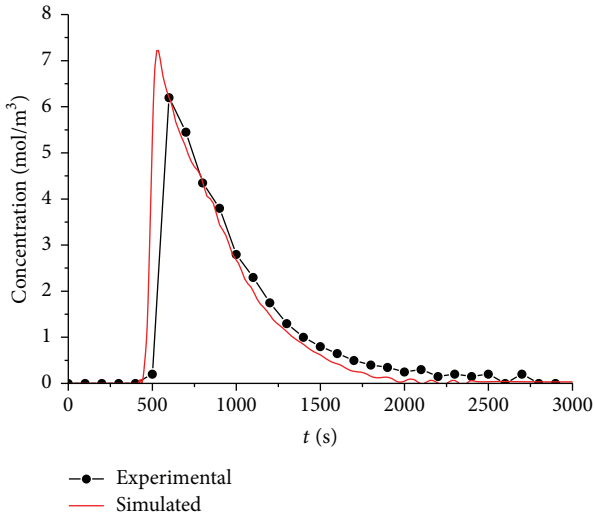

Figure 2: Verification of the integrated hydrodynamic and mass transfer models.

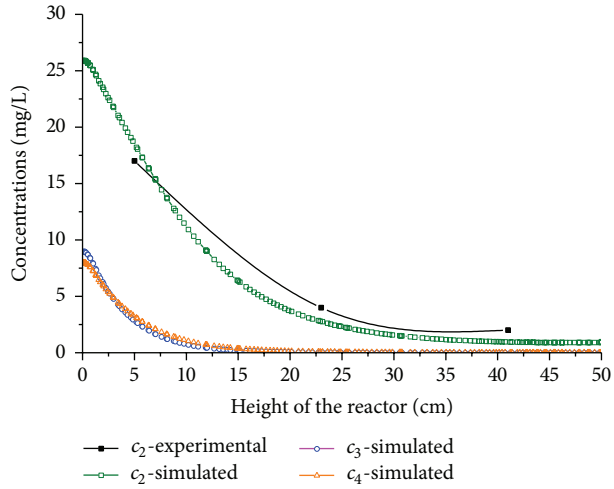

Figure 3: Verification of integrated hydrodynamic and biokinetics in sludge bed.

while an influent distribution plate was fixed at the bottom of the reactor and the reactor was filled with clean water.

While sludge presented in the reactor, tracer experiment was not performed because potential adsorption and precipitation of Ca^{2+} might result in loss of the tracer. LiCl is generally applied as a tracer in bioreactors. However, because analysis of Li^+ could not be performed while this research was carried out, tracer experiments were not performed while sludge presented in the reactor. Ca^{2+} concentrations were measured by standard method [17].

3. Results and Discussions

Figure 2 shows the Ca^{2+} concentrations obtained at the outlet of the EGSB reactor during the tracer experiment. Simulated Ca^{2+} concentrations matched experimental Ca^{2+} concentrations well, which indicates that the applied equations ((4)–(6), (9)) could be applied to model hydrodynamics and mass transfer in the reactor where no sludge presented.

VFA concentrations at sampling points located at reactor wall were shown in Figure 3. Although the influent total VFA concentrations were between 350 and 430 mg/L, the applied backflow largely diluted the influent VFA concentrations, which resulted in low real reactor influent VFA concentrations. Because propionate and butyrate concentrations at every sampling point (shown in Figure 3) were below detection limits of the two fatty acids (4 mg/L), propionate and butyrate concentrations could not be measured. In addition, almost all VFA were degraded in the sludge bed because no VFA could be detected at the outlet of the EGSB reactor.

Figure 3 shows that measured and simulated acetate concentrations matched well, which indicates that applied hydrodynamics and mass transfer as well as biokinetic models were acceptable. The majority of propionate and butyrate were degraded at the bottom of the reactor, while acetate was quickly removed in the sludge bed.

Moreover, Figures 2 and 3 indicate that hydrodynamics and mass transfer in the EGSB reactor could be modeled by ((4)–(9)).

Hydrodynamics is important for bioreactors, as shortcut flow can result in low reactor efficiency. As for high rate anaerobic bioreactors, shortcut flow indicates that local organic load can be much higher than an expected value and consequently result in a poor reactor efficiency. Therefore, influent distribution at the inlets of high rate anaerobic reactors is important for overall reactor efficiency [19].

Traditionally, modeling of an aerobic wastewater bioreactor relies on a hydrodynamic model that treats the reactor as a combination of a number of ideal reactors (CSTRs or plug flow reactors). Then, by the application of activated sludge models to each ideal reactor, effluent quality of a modeled reactor can be obtained. However, the construction of the hydrodynamic model is difficult and relies on experience [20]. Hydrodynamic models regarding anaerobic granular based reactors are much more complex than those regarding aerobic bioreactors [21], which makes modeling anaerobic bioreactors difficult. Alternatively, hydrodynamics can be modeled by a few equations ((4)-(5), (7)-(8)), which provides an accurate hydrodynamic modeling.

Figure 4 shows the distribution of influent at the bottom of the reactor. While a distribution plate was not applied (Figure 4(a)), influent could directly flow upwards with relative high velocity, which indicates that shortcut was incurred and reactor space was not fully utilized. While a distribution plate was applied (Figure 4(b)), though influent velocity near the middle of the distribution plate was higher than the surrounding liquid velocity, the influent was much more uniformly distributed in the entire reactor cross section. The sludge bed was a porous bed and provided flow resistance to the influent, which resulted in further improvement in influent distribution (Figure 4(c)). After flowing through the distribution plate, influent velocity immediately approached the required velocity, which indicates that a good influent distribution design was achieved.

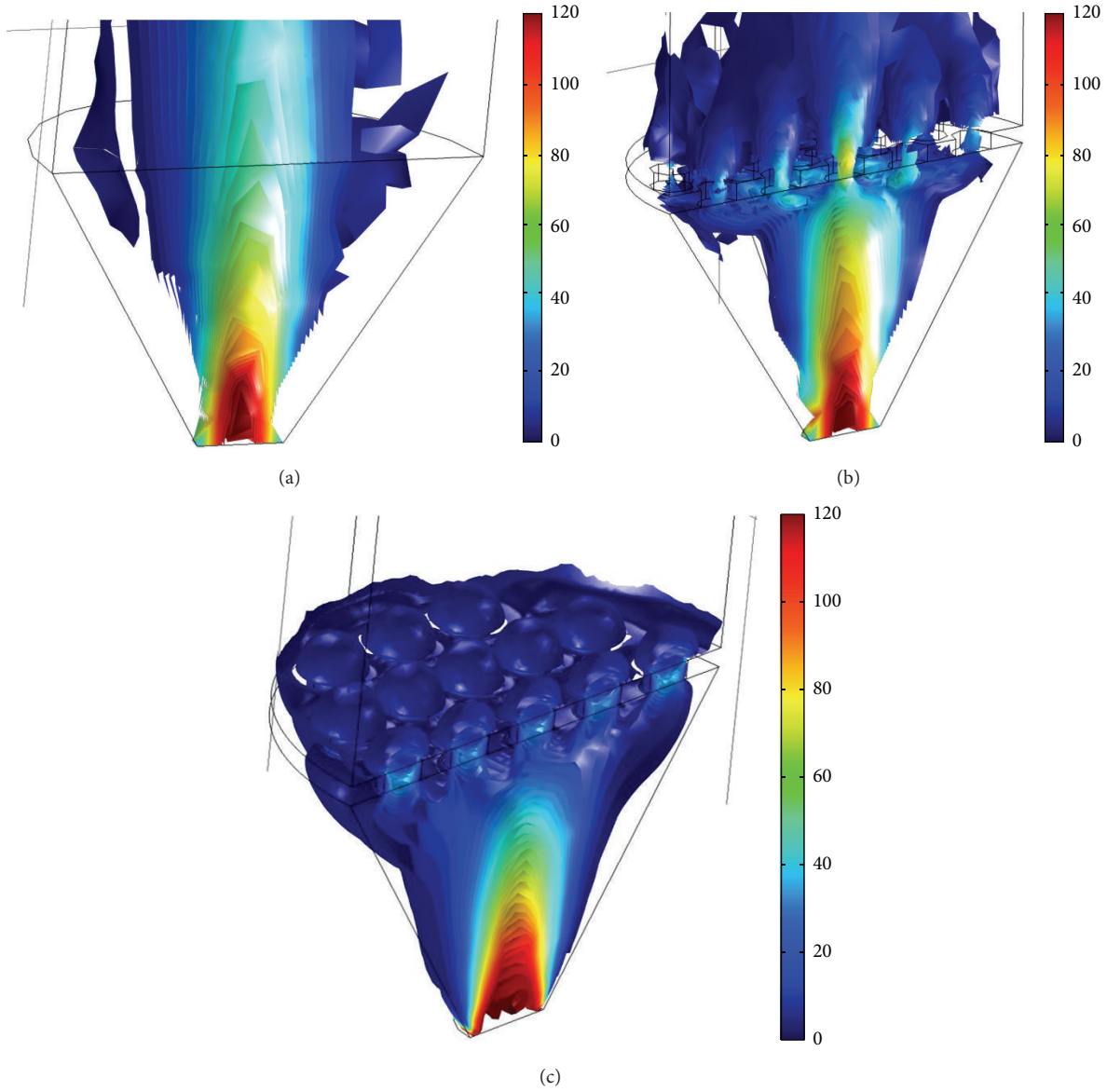

FIGURE 4: Influent distribution at the bottom of reactors (m/h). (a) No distribution plate and with clean water; (b) with distribution plate and clean water; (c) with distribution plate and sludge bed.

Up to now, relationships between operation parameters such as solid retention time, effluent quality, sludge activity, and microbial ecology variation have been well understood [1, 22–25]. However, many aspects such as reaction rates at each point in a reactor are hard to know as obtaining relative parameters at each point is not practical.

Figure 5 shows the VFA degradation rates in the sludge bed. The reaction rates of propionate and butyrate decreased along the flow direction in the reactor, which was different from that of acetate. The reaction rate of acetate increased and then decreased afterwards. That should derive from the conversion of butyrate and propionate into acetate, which resulted in a reaction peak. The distribution of reaction rates indicates that, due to the well influent distribution, a plug flow was well created in the reactor, which was beneficial for VFA degradation. Figure 5 also shows that VFA degradation rate distributions were different at each reactor cross section. VFA degradation rates near the reactor wall were lower than VFA degradation rates at the reactor axis, which is clearly shown in Figure 6. The maximum reaction differences were in the range of 0.2~0.4 mg/L·s. Nevertheless, the difference gradually decreased along the flow direction.

Reactor influents generally are provided by pumping that offers stable influent flow; therefore organic load fluctuation mainly comes from influent COD concentration variation, which results in effluent quality variation. When EGSB reactors are applied to municipal wastewater treatment, stability of effluent quality is interesting since influent COD level always fluctuates. The stability of the reactor was tested by providing a pulse COD load to the reactor in the model. The duration of the pulse COD load was 300 seconds. Influent COD increased from 300 mg/L to 600 mg/L, while influent

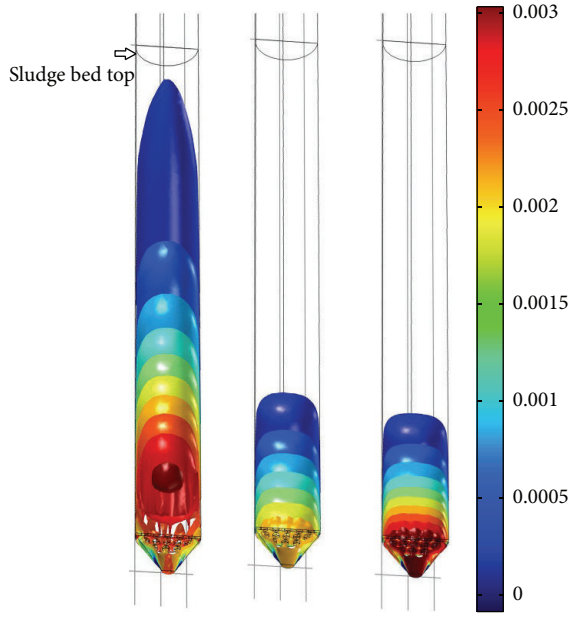

Figure 5: Distribution of VFA degradation rates in the EGSB reactor. From left to right: acetate, propionate, and butyrate (mg/L·s).

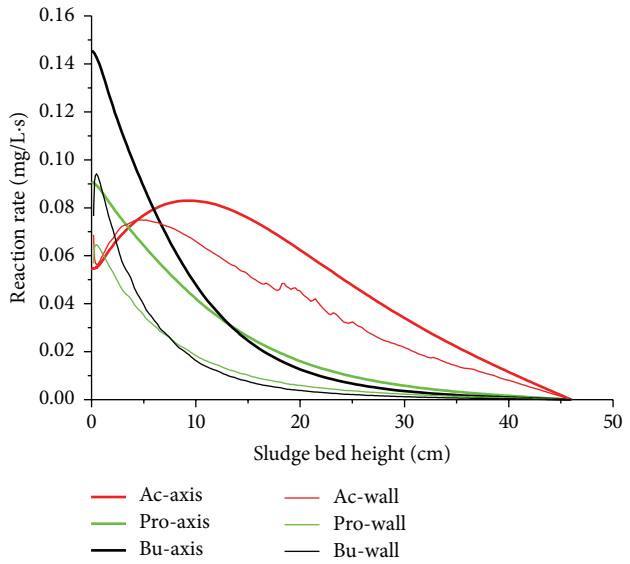

Figure 6: VFA degradation rates along sludge bed height at reactor axis (axis) and near reactor wall (wall) (mg/L·s).

flow velocity was constant. Figure 7 shows that the pulse COD load started and finished at 500 seconds and 800 seconds, respectively. The response of the pulse COD load showed that effluent VFA concentrations increased as the result of the influent COD pulse. However, VFA concentrations were still below the VFA detection limits. The butyrate concentration was quite low and Figure 7 can almost not show it. The stability test indicates that no matter how sharply COD load fluctuates, if COD load is always between 300 mg/L and 600 mg/L, the EGSB reactor could stably maintain VFA concentrations below the detection limits.

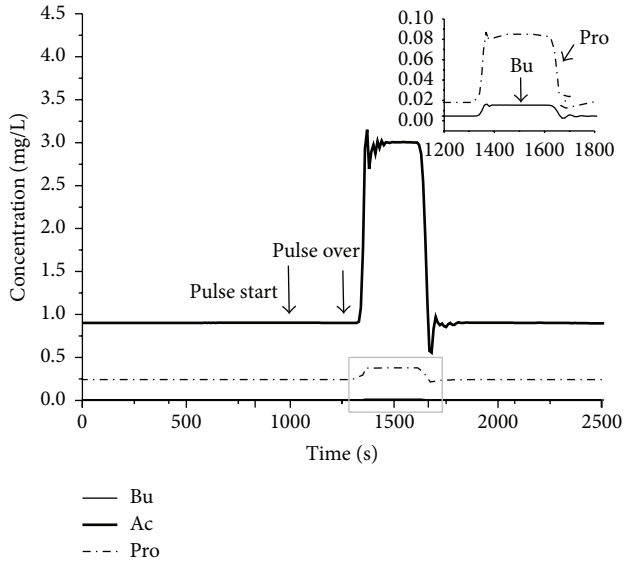

Figure 7: Effluent quality as a result of pulse COD loading.

4. Conclusions

A 3D CFD model was established, which included the effect of influent distribution in reactor hydrodynamics. In the model, the sludge bed in the reactor was treated as a porous bed, which was different from other publications that treated the sludge bed as a single phase that is different from water phase. Furthermore, the CFD model integrated biokinetics together, which could provide reactor operation details at different points in the reactor. Satisfactory modeling results regarding hydrodynamics and biokinetics were obtained. Based on this study, three conclusions can be obtained:

(1) The designed distribution plate could efficiently distribute influent at the bottom of the reactor, and the presence of sludge bed improved the influent distribution.

(2) The pulse increase of influent COD concentration from 300 mg/L to 600 mg/L had tiny impact on effluent quality, which showed good stability of the EGSB reactor.

(3) The degradation rate of acetate increased and then decreased along the flow direction in the reactor, while the reaction rates of propionate and butyrate decreased along the flow direction. VFA degradation rate distributions were different at each reactor cross section. VFA degradation rates near the reactor wall were lower than VFA degradation rates at the reactor axis.

Conflict of Interests

The authors declare that there is no conflict of interests regarding the publication of this paper.

Acknowledgments

Authors acknowledge the financial supports from the National Natural Science Foundation of China (no. 51408583), National Key Technology R&D Program (no. 2015BAD13B03), SRF for ROCS, SEM (no. Y43Z400O10), and Startup Foundation of CIGIT (no. Y33Z17N10) and Innovation and Entrepreneurship Leading Talent Program (no. Y33Z290O10).

References

[1] G. Lettinga, S. Rebac, and G. Zeeman, "Challenge of psychrophilic anaerobic wastewater treatment," *Trends in Biotechnology*, vol. 19, no. 9, pp. 363–370, 2001.

[2] V. O'Flaherty, G. Collins, and T. Mahony, "The microbiology and biochemistry of anaerobic bioreactors with relevance to domestic sewage treatment," *Reviews in Environmental Science and Biotechnology*, vol. 5, no. 1, pp. 39–55, 2006.

[3] S. Rebac, J. B. van Lier, P. Lens et al., "Psychrophilic anaerobic treatment of low strength wastewaters," *Water Science and Technology*, vol. 39, no. 5, pp. 203–210, 1999.

[4] J. B. van Lier, N. Groeneveld, and G. Lettinga, "Development of thermophilic methanogenic sludge in compartmentalized upflow reactors," *Biotechnology and Bioengineering*, vol. 50, no. 2, pp. 115–124, 1996.

[5] R. F. F. Pontes and J. M. Pinto, "Analysis of integrated kinetic and flow models for anaerobic digesters," *Chemical Engineering Journal*, vol. 122, no. 1-2, pp. 65–80, 2006.

[6] X. Wang, J. Ding, W.-Q. Guo, and N.-Q. Ren, "A hydrodynamics-reaction kinetics coupled model for evaluating bioreactors derived from CFD simulation," *Bioresource Technology*, vol. 101, no. 24, pp. 9749–9757, 2010.

[7] X. Wang, J. Ding, N.-Q. Ren, B.-F. Liu, and W.-Q. Guo, "CFD simulation of an expanded granular sludge bed (EGSB) reactor for biohydrogen production," *International Journal of Hydrogen Energy*, vol. 34, no. 24, pp. 9686–9695, 2009.

[8] B. Wu, "Computational fluid dynamics investigation of turbulence models for non-newtonian fluid flow in anaerobic digesters," *Environmental Science and Technology*, vol. 44, no. 23, pp. 8989–8995, 2010.

[9] B. Wu and W. Zhou, "Investigation of soluble microbial products in anaerobic wastewater treatment effluents," *Journal of Chemical Technology and Biotechnology*, vol. 85, no. 12, pp. 1597–1603, 2010.

[10] M. Brannock, Y. Wang, and G. Leslie, "Mixing characterisation of full-scale membrane bioreactors: CFD modelling with experimental validation," *Water Research*, vol. 44, no. 10, pp. 3181–3191, 2010.

[11] X. Wang, J. Ding, W.-Q. Guo, and N.-Q. Ren, "Scale-up and optimization of biohydrogen production reactor from laboratory-scale to industrial-scale on the basis of computational fluid dynamics simulation," *International Journal of Hydrogen Energy*, vol. 35, no. 20, pp. 10960–10966, 2010.

[12] B. Wu, "CFD investigation of turbulence models for mechanical agitation of non-Newtonian fluids in anaerobic digesters," *Water Research*, vol. 45, no. 5, pp. 2082–2094, 2011.

[13] B. Wu, "CFD simulation of mixing for high-solids anaerobic digestion," *Biotechnology and Bioengineering*, vol. 109, no. 8, pp. 2116–2126, 2012.

[14] J. Bridgeman, "Computational fluid dynamics modelling of sewage sludge mixing in an anaerobic digester," *Advances in Engineering Software*, vol. 44, no. 1, pp. 54–62, 2012.

[15] M. S. Vesvikar and M. Al-Dahhan, "Flow pattern visualization in a mimic anaerobic digester using CFD," *Biotechnology and Bioengineering*, vol. 89, no. 6, pp. 719–732, 2005.

[16] B. Wu, "Advances in the use of CFD to characterize, design and optimize bioenergy systems," *Computers and Electronics in Agriculture*, vol. 93, pp. 195–208, 2013.

[17] APHA, AWWA, and WEF, *Standard Methods for the Examination of Water and Wastewater*, American Water Works Association (AWWA) & Wat.Env.Fed.(WEF), Washington, DC, USA, 1998.

[18] J. Yang, H. Spanjers, and J. B. van Lier, "Non-feasibility of magnetic adsorbents for fouling control in anaerobic membrane bioreactors," *Desalination*, vol. 292, pp. 124–128, 2012.

[19] J. B. van Lier, N. Mahmoud, and G. Zeeman, "Anaerobic wastewater treatment," in *Biological Wastewater Treatment, Principles, Modelling and Design*, chapter 16, IWA Publishing, London, UK, 2008.

[20] D. J. Dürrenmatt and W. Gujer, "Automatic reactor model synthesis with genetic programming," *Water Science and Technology*, vol. 65, no. 4, pp. 765–772, 2012.

[21] V. Saravanan and T. R. Sreekrishnan, "Modelling anaerobic biofilm reactors—a review," *Journal of Environmental Management*, vol. 81, no. 1, pp. 1–18, 2006.

[22] R. K. Dhaked, P. Singh, and L. Singh, "Biomethanation under psychrophilic conditions," *Waste Management*, vol. 30, no. 12, pp. 2490–2496, 2010.

[23] G. Lettinga and L. W. Hulshoff Pol, "USAB-process design for various types of wastewaters," *Water Science and Technology*, vol. 24, no. 8, pp. 87–107, 1991.

[24] G. Lettinga, A. F. M. van Velsen, S. W. Hobma, W. de Zeeuw, and A. Klapwijk, "Use of the upflow sludge blanket (USB) reactor concept for biological wastewater treatment, especially for anaerobic treatment," *Biotechnology and Bioengineering*, vol. 22, no. 4, pp. 699–734, 1980.

[25] S. J. Lim and T.-H. Kim, "Applicability and trends of anaerobic granular sludge treatment processes," *Biomass and Bioenergy*, vol. 60, pp. 189–202, 2014.

[26] D. J. Batstone, J. Keller, I. Angelidaki et al., "The IWA anaerobic digestion model no 1(ADM 1)," *Water Science and Technology*, vol. 45, pp. 65–73, 2002.